Effect of Microwave Coupling and Magnetic Field Topology on Electron Temperature and Thrust on the Example of Two Electric Propulsion Concepts

C. E. Schäfer, J. Schmidt, F. Plettenberg, M. Grabe, Y. A. Chan, J. Martinez-Schramm, K. Bräumer, K. Holste, and P. J. Klar

Abstract Electric propulsion concepts involving electron cyclotron resonance excitation for plasma generation eliminate the need for electrodes inside the plasma. Concepts, employing magnetic nozzles to accelerate the entire plasma for thrust production, remove the necessity for a neutralizer. Two thruster concepts realizing such plasma production and acceleration are investigated: the well-known MINOTOR thruster prototype of ONERA and a new prototype under development at DLR called DEEVA. It is assumed that converging parts in the magnetic field lines along the plume direction lead to the weaker performance of the DEEVA prototype compared to the MINOTOR prototype. This study investigates the effects of magnetic field configurations on the DEEVA prototype, examining both a converging-diverging character and a strictly diverging configuration of the DEEVA magnetic field topology. The effects of these magnetic field variations are compared with the MINOTOR prototype using Langmuir probe measurements and thrust balance measurements. By observing trends resulting from operational variations of the prototypes - such as changes in input power, frequency settings, and volume flow - we can infer the influence of the magnetic field topology on plasma parameters and thrust. Potential improvements for thruster development are discussed based on the measured magnetic field topologies.

Keywords Electric propulsion · ECRT · Magnetic nozzle · Langmuir probe · Thrust balance

C. E. Schäfer (✉)
Propulsion Department, OHB System AG, Bremen, Germany
e-mail: clara.schaefer@ohb.de

J. Schmidt · F. Plettenberg · M. Grabe · Y. A. Chan · J. Martinez-Schramm
Spacecraft Department, German Aerospace Center, Göttingen, Germany

K. Bräumer · K. Holste · P. J. Klar
Institute of Experimental Physics I, Justus Liebig University, Giessen, Germany

M. Grabe et al. (eds.), *Rarefied Gas Dynamics*, Springer Aerospace Technology,
https://doi.org/10.1007/978-3-032-00094-1_63

1 Introduction

Typical issues with ion thruster technologies include electrode and grid erosion, along with the requirement for additional neutralizer devices [3]. Using electron cyclotron resonance (ECR) excitation for plasma generation, which eliminates the need for electrodes, offers a promising solution. Additionally, employing a magnetic nozzle (MN) to accelerate the entire plasma for thrust production removes the need for a neutralizer. The effects of electrodeless microwave coupling on plasma properties, combined with the magnetic field topology of a new thruster that achieves electrodeless plasma production and acceleration, are currently unknown. This study aims to fill this knowledge gap by comparing two thruster concepts. We examine the DEEVA (*DLR Electrodeless ECR Via microwave plasma Accelerator*) thruster, developed by the German Aerospace Center, which uses ECR for plasma production and a magnetic nozzle for acceleration. This is compared with a prototype of the well-known MINOTOR (*Magnetic Nozzle Electron Cyclotron Resonance Thruster*) concept, developed by the Office national d'études et de recherches aérospatiales (ONERA) [8]. Both prototypes employ a magnetic nozzle, are of similar size, and are designed to operate within a similar frequency and power range. However, they differ in terms of the concept employed for microwave coupling into the plasma as well as in the arrangement of the permanent magnets delivering the magnetic field topology. Comparing both thrusters under the same operating conditions (same power, volume flow and frequency setting) allows us to carry out detailed studies of the impact of the microwave coupling method and the magnetic field topology on plasma parameters.

As former studies have shown, the magnetic field topology of the DEEVA prototype includes a converging part in the magnetic field lines between the ECR zone and the thruster exit plane [11]. This is assumed to be the reason for the DEEVA prototype's performance not yet being comparable to the MINOTOR prototype [10, 11]. To investigate this assumption, we vary the magnetic field topology of DEEVA by realigning the permanent magnets. In one configuration, the disc magnets and the ring magnet are aligned in an attracting manner. This setup, referred to as *DEEVA-attractive*, was investigated in earlier studies [10, 11]. The second magnetic field setup aligns the magnets in a repulsive manner, and is therefore denoted as *DEEVA-repulsive*. In the repulsive configuration, a strictly diverging magnetic field character is expected. Previous studies have shown a correlation between electron temperature and ion energy for both the MINOTOR and DEEVA prototypes [5, 10]. This correlation is based on the assumption of an ambipolar electric field in the magnetic nozzle due to electron dynamics. Analyzing data from different diagnostic methods and directly comparing the plasma parameters of both thrusters enables us to assess the impact of different magnetic field configurations on performance.

2 Methods and Experimental Set Up

The experiments are conducted in the vacuum facility *Simulationsanlage für Treibstrahlen Göttingen - Miniatur Triebwerke* (STG-MT) at the DLR in Göttingen. The chamber has a length of 1 m and a diameter of 1.1 m. It is equipped with two backing pumps, a rotary vane pump, and a roots pump yielding a base pressure of 10^{-3} mbar. For lower pressure ranges a turbomolecular pump is added allowing pressure ranges of 10^{-6} mbar and background pressures during thruster operation in the range of 10^{-5} mbar. For the operation of the thrusters, we use the microwave signal generator KU-SG 2.45-250A of the company Kuhne Elecronics GmbH as well as the Bronkhorst mass control unit (MCU) for maximum 50 sccm air. The gases in use are xenon, in case of MINOTOR, and argon, in case of DEEVA. The mapping of each thruster is performed as follows: For all operation points the plasma is measured with Langmuir probe (LP) in $d = 100 \pm 0.5$ cm distance to the thruster exit. The thrust is investigated by means of thrust balance (TB) measurements. Multiple measurements performed at the same thruster setting using both the LP and the TB yield the experimental uncertainty in the results.

The operating principle of both the ECR thrusters with MN is the ionization of the propellant via ECR and the acceleration by a divergent magnetic field [2, 8, 14]. The prototypes are described in various publications [9, 10]. In presence of a magnetic field, charged particles (electrons and ions) are trapped along the magnetic field lines in such a way that they are circulating (gyrating) around the field lines, due to Lorentz forces [14]. If an electromagnetic wave with that cyclotron frequency is applied, the electron is resonantly accelerated by the electric field of the wave. It absorbs the energy of the electromagnetic wave, gains kinetic energy and increases the impact ionization process rate [2, 14]. Given the magnetic field of 87.5 mT, one comes to a microwave frequency of 2.45 GHz for resonant excitation. The acceleration of the produced ions is due to the gradient in the magnetic field strength. The magnetic moment μ of the charged particles (forming due to the gyration of the particles about the magnetic field lines) and the mass of the particle m, can be used to formulate an acceleration ($\dot{v}_{||}$) opposite to the gradient direction $\nabla_{||} B$ [6, 14]:

$$m\dot{v}_{||} = -\mu \nabla_{||} B. \tag{1}$$

The electrons therefore experience a force in opposite direction of the gradient in magnetic field strength, leading to a charge separation and the build up of an ambipolar electric field. It is a well-established assumption of MN's, that this electrostatic field converts the thermal energy motion of the electrons into ion kinetic energy. Therefore the electron dynamics plays a crucial role in configuring the electrostatic field in the plume, responsible for ion acceleration and ultimately thrust generation [4].

The magnetic field plays a crucial role in the functioning of the thruster, more specifically in the generation and acceleration of the quasi-neutral plasma. For this reason, the thruster's magnetic field is measured in three spatial directions using a

3D Hall probe from the company Projekt Elektronik GmbH. The range of the probe in use is ±200 mT and the linearity error is given as ±0.1 mT. In addition to the downstream measurements, the magnetic field in the vicinity of the ECR zone is also measured. This is possible by moving the probe in all three spatial directions (x, y, z) with linear stages. We will present results in the x, y plane after confirming rotational symmetry.

One of the most technically simple, yet difficult to interpret, diagnostics tools is the Langmuir probe (LP) [14]. A single electrode probe is introduced into the plasma and the voltage U is varied with respect to a reference potential. The current-voltage characteristic obtained, delivers a set of plasma parameters. For this study the crucial electron energy distribution function EEDF ($f(E)$)—based on the second derivative of the measured current voltage characteristic $\frac{\mathrm{d}^2 I_\mathrm{e}}{\mathrm{d}U^2}$ is determined [1]. By taking the moment of the distribution function we obtain the electron temperature T_e of the plasma:

$$T_\mathrm{e} = \frac{2}{3n_\mathrm{e}} \int_0^\infty f(E)\, E\, \mathrm{d}E. \tag{2}$$

The thrust balance DEPB (*DLR Electric Propulsion Thrust Balance*) used in this investigation is described in Refs. [7] and [13]. It is an inverted double pendulum, consisting of two pendulums connected by a plate with a given stiffness and elasticity. The TB consists of an aluminium table, casing and eight quartz-glass rods used as flexible bearings for the thruster table. To dampen possible high frequency oscillations an eddy current brake is built in. A micrometer-screw is used to establish the connection between the moving thrust balance table and the Sartorius® WZA224 load cell [13]. An accuracy of 0.2 mN and a repeatability of 0.1 mN for the DEPB are given [12]. In our study, multiple measurements are conducted for each operation point of the thruster to determine the mean thrust based on delta measurements. A "delta measurement" involves running the thruster for several minutes and then switching it off. The resulting step change in the force measurement curve is identified as the produced thrust. This process is repeated multiple times, and the thrust values are averaged. The standard deviation of these values is represented as error bars in the following.

3 Magnetic Field and Plasma Characteristics

The three magnetic field configurations can be seen in Fig. 1. The ECR zones, where a magnetic field strength of $|\vec{B}| = 87.5$ mT is achieved, is marked by a white line for all three configurations. For all three set ups, $x = 0$ marks the thruster exit plane. As one can see in case of MINOTOR the ECR condition is achieved close to the back plate. The magnetic field then decreases fast, leading to a high gradient in magnetic field strength. In case of DEEVA-attractive, a diverging-converging-diverging character

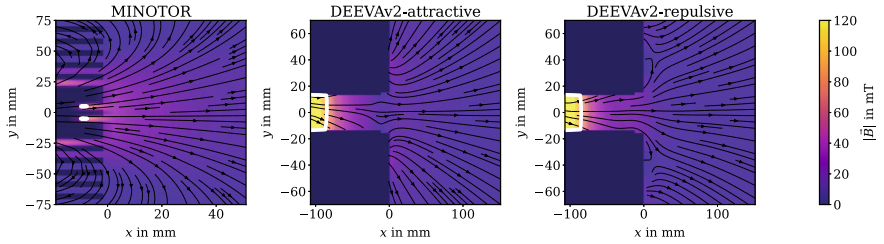

Fig. 1 Magnetic field configurations of the ECR thrusters. **a** MINOTOR is pictured on the left, dark area at $x < 0$ marks the mask where the probe could not access the thruster. $x = 0$ marks the thruster exit plane. The white dots mark the magnetic field strength of $|\vec{B}| = 87.5\,\mathrm{mT}$, the ECR zone. DEEVA in the center is shown in attractive configuration (**b**). On the right DEEVA is shown in repulsive configuration (**c**). Again, the dark area at $x < 0$ marks the mask where the probe could not access the slotted antenna. $x = 0$ marks the thruster exit plane and the white line $|\vec{B}| = 87.5\,\mathrm{mT}$, therefore the ECR zone

of the magnetic field can be observed. Since the converging part could lead to a reflection of particles, it is decided to test a different magnetic field configuration; the DEEVA-repulsive configuration is depicted in Fig. 1 on the right. Here we see again, the ECR condition is fulfilled in the back of the thruster vessel, near to the gas inlet. In contrast to DEEVA-attractive, we observe in this configuration a strictly diverging character of the magnetic field lines.

The effect of magnetic field topologies on the electron temperature with changes in operational points is shown in Fig. 2. On the left, we see the input power variation. The center plot shows the frequency variation, and the right plot depicts the variation in volume flow. The electron temperature for the MINOTOR prototype is higher across all operational parameter variations. For the two DEEVA configurations, DEEVA-attractive and DEEVA-repulsive, the repulsive configuration shows higher values in both power and frequency variations. For power variation, there is not a significant change in electron temperature for all prototypes. However, for frequency variation, higher values are observed around the design frequency of 2450 MHz for MINOTOR (a) and DEEVA-repulsive (c). In contrast, DEEVA-attractive (b) shows little change with frequency variation. For all three prototypes, electron temperature decreases with increasing volume flow. The values for the DEEVA-attractive configuration are the lowest, while those for the MINOTOR are the highest.

As shown in Fig. 3, the overall thrust for the MINOTOR prototype is higher, reaching up to $T_\mathrm{T} = 1.7\,\mathrm{mN}$. In contrast, the thrust values for both magnetic field topologies of the DEEVA thruster do not exceed 0.3 mN. There is no significant difference in thrust between the two DEEVA configurations. We observe an increase in thrust for all three prototypes with increasing input power. For MINOTOR, there is a clear optimum at 2450 MHz. DEEVA-attractive also shows an optimum at this frequency. DEEVA-repulsive operates at a constant thrust value over a broader frequency range. For volume flow variation, thrust decreases with increasing volume flow for all prototypes. However, DEEVA-attractive shows a slight increase in thrust around 2 sccm before decreasing as well.

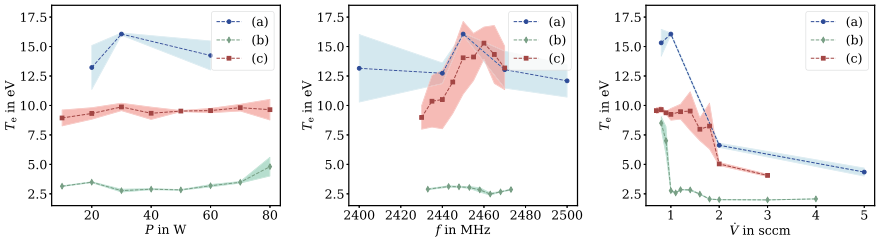

Fig. 2 Comparison between the determined electron temperatures T_e for the MINOTOR (**a**), DEEVA-attractive (**b**) and DEEVA-repulsive (**c**) configurations. The plot on the left shows power variations at a frequency set of 2450 MHz and a volume flow of 1 sccm of argon (in case of DEEVA) and xenon (in case of MINOTOR). The center plot depicts frequency variation at power input of 30 W and a volume flow of 1 sccm. The right plot shows the volume flow variation (of again argon, in case of DEEVA; and xenon, in case of MINOTOR) at the constant frequency 2450 MHz and input power of 30 W. The filled space shows the standard deviation of the resulting values from multiple measurements

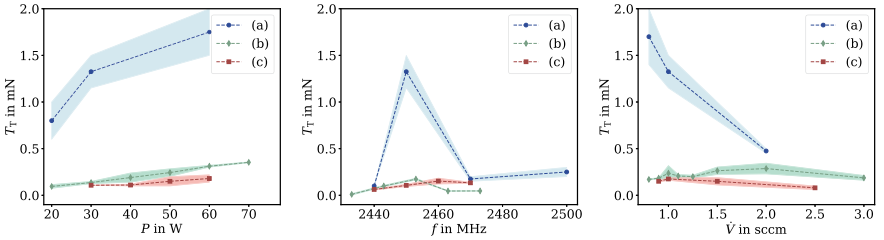

Fig. 3 Comparison between the determined thrust T_T for the MINOTOR (**a**), DEEVA-attractive (**b**) and DEEVA-repulsive (**c**) configurations. The plot on the left shows power variations at a frequency set of 2450 MHz and a volume flow of 1 sccm of argon (in case of DEEVA) and xenon (in case of MINOTOR). The center plot depicts frequency variation at power input of 30 W and a volume flow of 1 sccm. The right plot shows the volume flow variation (of again argon, in case of DEEVA; and xenon, in case of MINOTOR) at the constant frequency 2450 MHz and input power of 30 W. The filled space shows the standard deviation of the resulting values from multiple measurements

4 Discussion

First and foremost, it is important to note that MINOTOR is operated with xenon, while both DEEVA configurations are operated with argon. This choice is based on preliminary measurements showing significantly higher ion energies when DEEVA attractive is operated with argon [10]. This comparative study must be considered in light of this difference. Xenon is heavier than argon, and thus, the same ion energy results in higher thrust for xenon. Measurements of the magnetic field topologies revealed that the DEEVA-repulsive configuration indeed achieves a strictly diverging magnetic field. The higher gradient observed after the thruster exit in MINOTOR should result in greater electron acceleration (see Eq. 1). With the changes in magnetic field topology in the DEEVA-repulsive case, aiming for high gradients while avoiding

excessive convergence in magnetic field lines, we achieve higher electron temperatures compared to the attractive configuration, and they are almost comparable to those of the MINOTOR prototype.

We can consider possible explanations for our findings that the determined thrust is not significantly higher in the DEEVA-repulsive configuration compared to the DEEVA-attractive configuration and not as high as in the MINOTOR case, despite the higher electron temperatures suggesting otherwise. Firstly, the ion energies must be investigated and correlated with the electron temperatures presented in this study. Secondly, the ion current, which determines the total number of ions ejected from the thruster need to be determined. The third explanation involves thrust generated by neutral gas. Alongside investigating ion energy and ion current to determine thrust production, it's crucial to consider the effects of neutral gas on thrust. As reported in Ref. [15], thrust calculated using probe measurements underestimates total thrust. By comparing calculated thrust with thrust balance results, we can estimate the efficiency of the magnetic nozzle designs employed in this study.

Due to the early development stage of the new DEEVA thruster, it is uncertain whether it can achieve performance levels comparable to the optimized MINOTOR thruster in the future. However, the DEEVA concept introduces electrodeless microwave coupling into the plasma and electrodeless acceleration with a magnetic nozzle, potentially paving the way for long-term space missions employing ECR thrusters.

References

1. Demidov V, Ratynskaia S, Rypdal K (2002) Electric probes for plasmas: the link between theory and instrument. Rev Sci Instrum 73(10):3409–3439
2. Goebel D, Katz I (2008) Fundamentals of electric propulsion: ion and Hall thrusters, vol 1. Wiley
3. Holste K, Dietz P, Scharmann S, Keil K, Henning T, Zschätzsch D, Reitemeyer M, Nauschütt B, Kiefer F, Kunze F et al (2020) Ion thrusters for electric propulsion: Scientific issues developing a niche technology into a game changer. Rev Sci Instrum 91(6):061101
4. Kim J, Chung KJ, Takahashi K, Merino M, Ahedo E (2022) Kinetic electron cooling in magnetic nozzle: experiments and modeling. Plasma Sources Sci Technol
5. Lafleur T, Cannat F, Jarrige J, Elias P, Packan D (2015) Electron dynamics and ion acceleration in expanding-plasma thrusters. Plasma Sources Sci Technol 24(6):065013
6. Longmier B, Bering E, Carter M, Cassady L, Chancery W, Díaz FC, Glover T, Hershkowitz N, Ilin A, McCaskill G et al (2011) Ambipolar ion acceleration in an expanding magnetic nozzle. Plasma Sources Sci Technol 20(1):015007
7. Neumann A, Simon J, Schmidt J (2021) Thrust measurement and thrust balance development at dlr's electric propulsion test facility. EPJ Techn Instrum 8(1):17
8. Packan D, Elias P, Jarrige J, Vialis T, Correyero S, Peterschmitt S, Porto J, Merino M, Sánchez-Villar A, Ahedo E et al (2019) H2020 minotor: magnetic nozzle electron cyclotron resonance thruster. In: 36th international electric propulsion conference
9. Peterschmitt S, Packan D (2019) Comparison of waveguide coupled and coaxial coupled ecra magnetic nozzle thruster using a thrust balance. In: IEPC 2019

10. Schaefer C, Schmidt J, Plettenberg F, Chan Y, Grabe M, Marinez-Schramm J, Holste K, Klar PJ (2024) Comparative study of electron temperature and ion energy in two different magnetic nozzle thruster designs. In: 39th international electric propulsion conference
11. Schaefer C, Schmidt J, Plettenberg F, Chan Y, Grabe M, Marinez-Schramm Heinz TJ, Holste K, Klar PJ (2024) Investigation of the correlation between microwave coupling and ion energy on the example of two thruster concepts. In: Space propulsion conference
12. Schmidt J (2023) DLR electric propulsion balance documentation
13. Schmidt J, Simon J, Neumann A (2022) Thrust measurements of the rit-10 thruster with dlr's new depb thrust balance. In: 8th international conference on space propulsion, pp 1–7
14. Stroth U (2011) Plasmaphysik. Springer
15. Vialis T, Jarrige J, Aanesland A, Packan D (2018) Direct thrust measurement of an electron cyclotron resonance plasma thruster. J Propuls Power 34(5):1323–1333